Article

From laser scanning to finite element analysis of complex buildings by using a semi-automatic procedure

Giovanni Castellazzi[1,*]**, Antonio Maria D'Altri** [1]**, Gabriele Bitelli** [1]**, Ilenia Selvaggi** [1] **and Alessandro Lambertini** [1]

[1] Department of Civil, Chemical, Environmental, and Materials Engineering (DICAM), University of Bologna, V.le Risorgimento 2, Bologna, Italy

* Author to whom correspondence should be addressed; giovanni.castellazzi@unibo.it, +39 051 2093503, +39 051 2093496

Abstract: In this paper a new semi-automatic procedure to transform three-dimensional point clouds of complex objects to three-dimensional finite element models is presented and validated. The procedure (*CLOUD2FEM*) conceives the point cloud as a stacking of point sections. The complexity of the clouds is arbitrary since the procedure is designed for terrestrial laser scanner surveys applied to buildings with irregular geometry, such as historical buildings. The proposed method allows to always produce a *filled* three-dimensional model ready to use for structural analysis purpose. A comparison analysis with a CAD based model is carried out on a historical building damaged by a seismic event.

Keywords: Terrestrial Laser Scanning; Historical buildings; Geometric modeling; Finite element analysis; Structural analysis; Cultural Heritage

1. Introduction

Terrestrial Laser Scanner (TLS) surveys allow to produce a fine geometric representation of objects by means of accurate dense clouds of 3D points belonging to the surface, plus additional information such as the intensity of the reflected signal, the color etc. These features make this kind of survey very useful when a "snapshot in time" is needed to freeze the status of the object. This concept has been applied very often within the field of Cultural Heritage to support multidisciplinary studies: from

simple documentation, monitoring of the condition of the building, as support for restoration works or for structural analysis checks. Consider for instance the possibility to capture, by means of an orthophoto derived from digital pictures and 3D surveys, the degeneration of the building condition such as the one produced by the presence of moisture content.

TLS can be used for damage assessment in post-earthquake surveys, where the damage of buildings is widespread. In this situation TLS can be applied also to internal parts of the building, not being limited only to the external façades as usually happens. Within this context the present study aims at introducing a new semi-automatic procedure to generate a Finite Element (FE) model from a Laser Scanner survey of a building.

The problem of automatic transformation of large point cloud dataset to simplified geometrical object is a well known and studied topic. Several contribute are available in literature and some of them propose semi automatic procedure specialized for specific use. In the context of Airborne Laser Scanner (ALS) the automatization aim at reconstructing simplistic shapes of buildings to use with projection textures from terrestrial and airborne images. Consider for instance [1] where an approach for automated generation of building models from ALS, comprising the entire sequence from extraction to reconstruction and regularization is presented, or [2] where the 3D simplified modeling of buildings is finalized to a study about solar radiation potential. Recently, in the field of Civil Engineering, laser scanner surveys are gaining particular interest to generate structural models, since the increasing computational capabilities allow to manipulate large datasets. The automation here aims at reconstructing precisely the building's complexity by its main geometric features. Several are the studies available in the literature, but in some cases the cloud is simple or dramatically simplified. In [3] a pipeline to reconstruct complete geometry of architectural buildings from point clouds obtained by sparse range laser scanning is presented for architectures that are made of planar faces. The proposed technique faithfully constructs a polyhedron of low complexity based on the incomplete scans, but do not resolve fine geometry details. In [4], a three-dimensional cloud of point is used to generate a cross sections model to be used for structural analysis application, while in [5] an example of FEM analysis of a whole building is carried out using laser scanning data. In [6] it is presented a methodology to estimate the deformation of arches or vaults based on the symmetry of sections obtained along the vault guideline. Even here the accurate geometry of the masonry arches is obtained by means of a three-dimensional laser scanner survey, reduced to the inner arches surfaces representation. Massive structures, such as masonry bridges can also be investigated by summing the laser scanner survey information to those obtained by ground penetrating radar obtaining a fine picture of the external and internal feature [7]. Here the cloud simplification lies on the sampling of some points useful to reconstruct the geometry by means of regular geometry.

More interesting for this paper is the contribution proposed in [8]-[9], that try to precisely catch the building geometry by automatic reconstruction of its boundary. Consider for instance the contribution given in [10] where a point-based voxelization method to automatically transform point cloud data into solid models for computational modeling is presented. The method basically construct a Triangular Irregular Network (TIN) mesh and then by means of a voxel grid bounds the cloud region. The resulting model is capturing the three-dimensionality of the survey but do not capture the whole structure since is designed for façade structures [8]-[9].

In this paper we present and validate *CLOUD2FEM*: a new semi-automatic procedure to transform three-dimensional point clouds of complex objects to a three-dimensional finite element model. The procedure conceives the point cloud as a stacking of point sections. The point cloud used in our case study for the procedure validation was acquired with TLS survey.

Our procedure requires to start with a previously acquired dataset: consider for instance, within the cultural heritage scope, a survey thought to document a historical building, to support restoration works or to permit simple direct structural evaluation.

The complexity of the clouds is arbitrary since the procedure is designed for terrestrial laser scanner surveys of buildings with irregular geometry, such as historical buildings. It should be stressed, however, that this procedure does not require a particular methodology of acquisition of the cloud, which is therefore not limited to TLS, but can be obtained using digital photogrammetry or any other suitable technique.

As previously said, the TLS data output can reach an high level of detail and has to be synthesized to produce a data input for FE modeling. This operation is not trivial, because the simplified model must retain all the information regarding the structural elements. The proposed method allows to always produce a *filled* model ready to use for structural analysis purpose.

The paper is organized as follows: Section 2 presents the proposed procedure and illustrates its potential by means of a simple application; Section 3 presents the validation of the procedure by its application to a complex historical monumental building: a structural analysis of the building is presented and discussed by comparing the finite element model obtained with the proposed procedure with a CAD based finite element model. Some concluding remarks end the paper.

2. Proposed method

Given an accurate description of a complex geometry, for instance consider a point cloud as Figure 1(a) - 1(b), our procedure allows the reconstruction of the original three-dimensional geometry by means of a particular discretization.

In order to apply the procedure some preliminary (common) operations may be required to improve the reconstruction quality and reduce the error propagation due to the stitching of large and complex point clouds. The point clouds can rarely be directly transformed into a filled and complete 3D model without user intervention: complex shape of the geometry, spatial points irregularly distributed, missing faces are critical aspects which usually prevents the automation of the process.

2.1. Slices Generation from Point Cloud Survey

TLS is an optical instrument that allows the survey of an object in its three-dimensional coordinates through subsequent scans. The scanner sweeps sistematically the space with the measurements until it has a complete picture of the surrounding three-dimensional space. A laser scanner provides a three-dimensional coordinates system as a direct result: a high number of points that are hit by the laser pulse. All these measurement generate a point cloud, which describes the external surface of the scanned object.

The scanner laser is one of the three-dimensional active measurement systems. In particular ranging scanners are used for architectural surveys, thanks to their direct measurement of the distance up to hundreds of meters. They are divided into Time Of Flight (TOF) and phase based measurement. The first method is based on measuring the transit time of a short laser pulse to an optical visible target and back to the receiver. The phase based measurement sends a pulse modulated by an harmonic wave. The distance in this case is calculated by comparing the phase difference between the emitted wave and the received one.

A ranging scanner is very efficient: it can record hundreds of thousands of points per second, and can achieve an accuracy in the order of few millimeters on the coordinates of the single points. A typical TLS survey is composed from subsequent stages. The first is the planning and it depends on the specific object to survey. It determines the various positions of the instrument (*scan positions*), based on a good overlap between scans and in order to avoid undetected areas, and to obtain a proper density according to different parameters. The following phase is to properly position the targets, i.e. control points in common between adjacent *scan positions*, used to merge all the point clouds acquired in a unique three-dimensional model. In a survey of a large complex building, an accurate three-dimensional topographic survey georeferencing each target is critical to the success of the procedure, in order to reduce the error propagation derived from stitching together a large number of point clouds, each one in its own local reference system. Fulfilled all the previous requirements, it's possible to acquire the data with TLS instrument, in the various scan positions previously determined. At the same time it is useful to obtain optical images as an integration of the point clouds. A software is then used to process the data surveyed and to align and merging all the point clouds. The robustness of the alignment can be enhanced using known coordinate from the acquired targets, producing a unique, optimized point cloud.

Point clouds slicing is a common procedure to extract sections and details from large point clouds database. CAD based procedures are often used to transform sliced points into *line-based* models. Upon this condition we conceive the point cloud as a stacking layer sequence of "planar points". In Figure 1 a simple geometry is illustrated and referenced to the cartesian system, where the axis Z is the principal direction of the stacking sequence (Figure 1(c)). The structure is subdivided by subsequent section planes Π_j^z, each one characterized by an incremental z-coordinate of Δz. Then all the points within the range $[z_j - \Delta z/2, z_j + \Delta z/2]$ are projected to the mid-plane Π_j^z (see Figure 1(d)).

Within a software for the management of spatial referenced data (e.g. a GIS, Geographic Information System) we can manipulate the points belonging to each section of Δz thickness and generate the pattern of points located on the Π_j^z plane. This model is composed from slices of the model at constant steps and the distance between two adjacent slices has to be chosen accordingly to the final resolution of the FE model. A sequence of points at a constant interval and high density are placed along the lines contained in each slice.

In this way we scale down a three-dimensional problem to a two-dimensional problem, because each slice contains only points with variable (x, y) coordinates and a constant z_j coordinate. A boundary polygon that encloses the points can be computed using a concave or convex hull algorithm [11]. Then further manipulation is done by a in-house Python script that walks through the dataset, with a parsing technique, and separates points belonging to each slice.
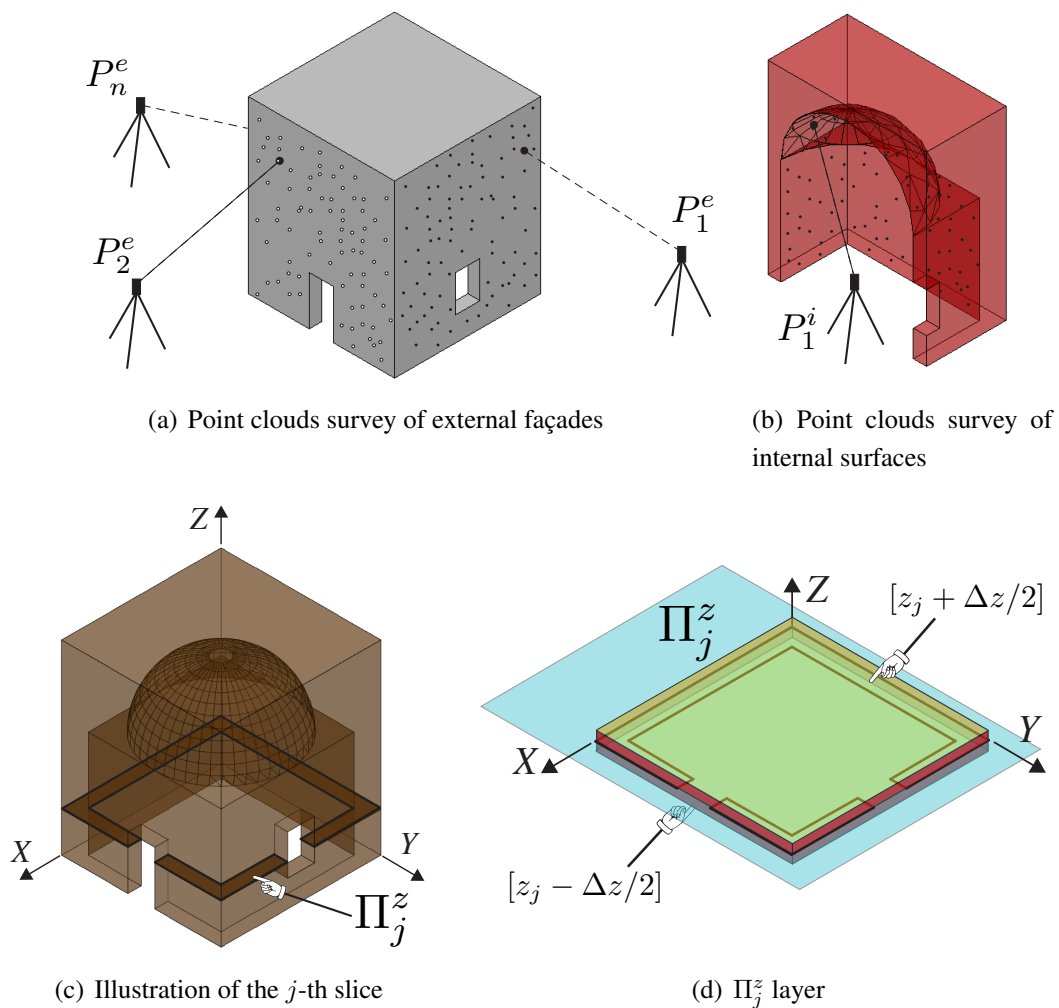
(a) Point clouds survey of external façades

(b) Point clouds survey of internal surfaces

(c) Illustration of the j-th slice

(d) Π_j^z layer

Figure 1. Visualization of the stacking layer sequence concept.

In case of a building, the slices contain two principal profiles: the first made by connecting the points that belong to the external point cloud (consider for instance the survey of the external facade of a building, see Figure 1(a)) and the second made by connecting the points that belong to the internal point cloud (consider for instance the survey of the internal rooms of a building, see Figure 1(b)).

The first gives as output a filled geometry that we call *external* because envelops the whole building. It may be composed of several *islands* all representing the outside face of the building walls.

Similarly, the second produces a boundary polygon called *internal* that is computed selecting only the points acquired in the internal rooms. It is important to emphasize that also this polygon, in the same way as the *external*, is created using a concave hull algorithm [12], enveloping the point selection from the outside. Also this polygon may be composed of several *islands* representing the various rooms of the building.

Now we have two polygons, one external and one internal, and both have a filled geometry. Subtracting the second from the first we obtain our first result: a filled polygon for each slice of the building that describes the entire structure.

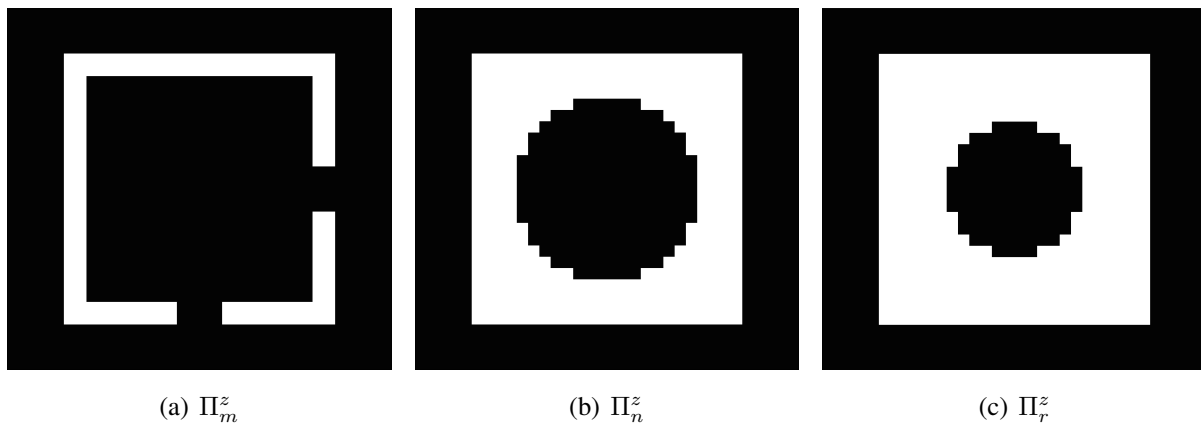## 2.2. Finite Element model Generation from Slices

(a) Π_m^z (b) Π_n^z (c) Π_r^z

Figure 2. Two dimensional images obtained by slicing the structure illustrated in Figure 1: m, n and r represent three generic slices located at z_m, z_n and z_r coordinates respectively.

Once the slices have been created we need to introduce the discretization procedure in order to set up the desired FE model. Here we propose to discretize first the two-dimensional sections and then to use them to build the three-dimensional dicretized model. By using the Computed Tomography (CT) approach [13], each slice has been idealized as a digital image, with a certain resolution, composed of picture elements (pixels) so the stacking of these slices generate the volume elements (voxels). This procedure allows to reconstruct the original three-dimensional geometry by stacking all of its slices, so a complete volumetric representation of the object is obtained by acquiring a contiguous set of slices.

The original polygon is then described by a $N \times M$ pixel matrix corresponding to a grid of pixel with a particular resolution. With reference to Figure 2 the pixel value will be for instance, in a eight-bit gray scale, 255 for filled area and 0 for empty spaces. This transformation is performed automatically for each slice with a fixed region preserving the output resolution. In this way all the grids are aligned and we build the voxel model stacking them in the original order, following their coordinates. It is worthy to underline that the voxels are not placed along the internal and external profiles as proposed by other techniques [8]-[10].

Voxels, as represented in Figure 3(a), define a particular grid structure that posseses the following features:

- Π_j^z planes are chosen with normal along Z that is the building construction direction: features, layers, openings are conceived by a stacking of elements (i.e. bricks) along the Z direction;

- Δz is chosen accordingly to the building complexity along the Z direction;

- Δx and Δy are chosen accordingly to the in-plane complexity and are totally indipendent from Δz;

- The stacking procedure is here proposed as a linear stacking of contiguous slices but can be, in general, considered as interpolated along the Z direction (i.e. considering more slices at a time);

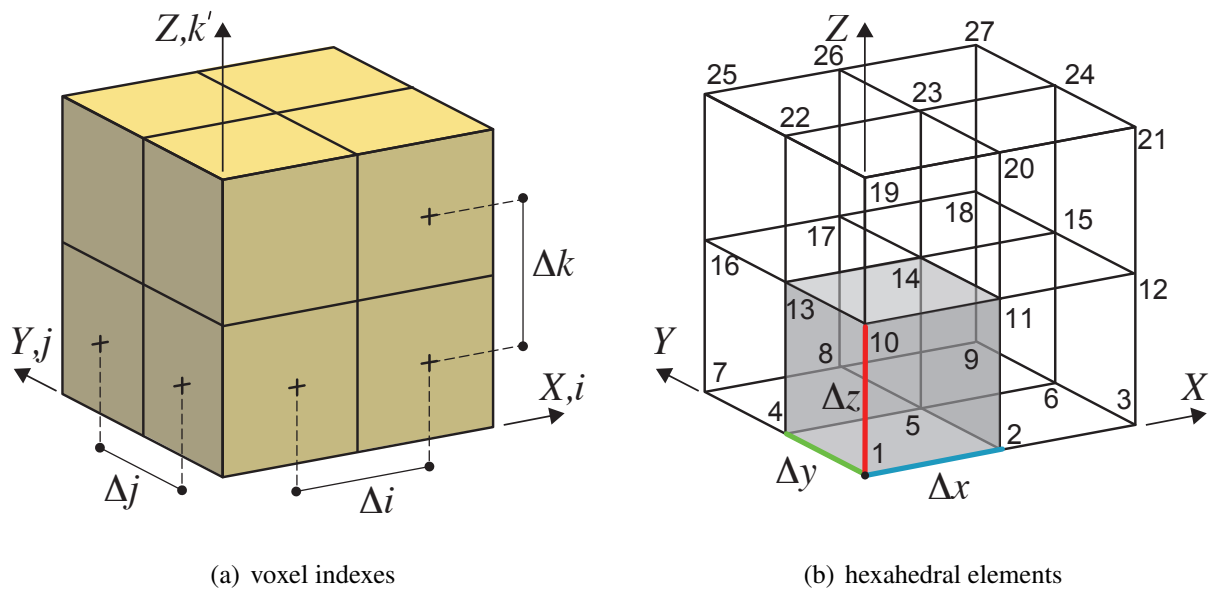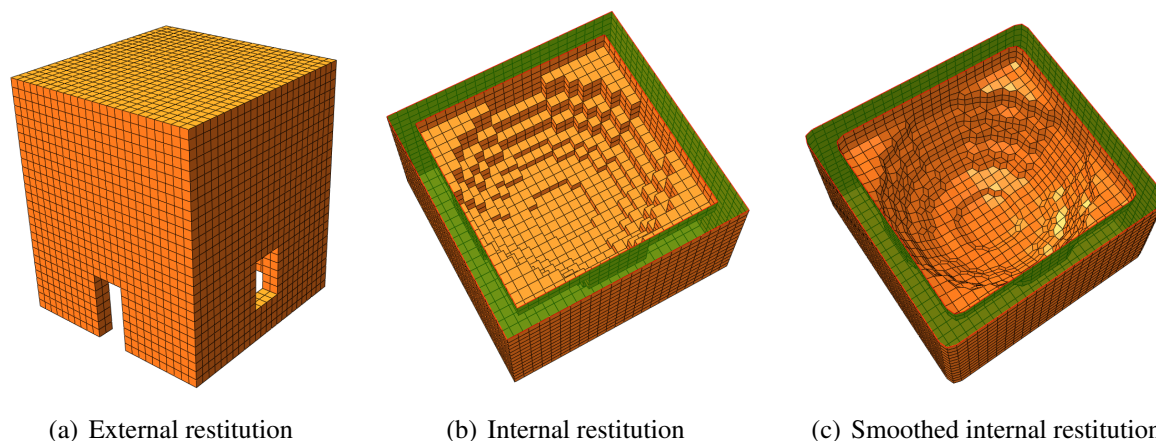- The resulting discretized volume does not need any particular further adjustment "to fill" the structure.

(a) voxel indexes (b) hexahedral elements

Figure 3. Voxel representation and finite element transformation: $\{i,\ j,\ k\}$ and $\{X,\ Y,\ Z\}$ are the indexes of the voxels three-dimensional matrix and the global coordinates of the structure respectively. The coordinate k' means $k' = R - k$ where R is the third size (along Z) of the voxels three-dimensional matrix ($N \times M \times R$).

The resulting dataset is simple and easy to use with finite element technique: each voxel is automatically transformed into an eight-node hexahedral finite element. By using a common space-partitioning data structure (KD–TREE), the scheme represented in Figure 3(a) is transformed in a Finite Element structure (Figure 3(b)) by simply generating the connectivity structure of each element.

In theory this operation can be performed for each voxel value (in this case 0 or 255) or only for a certain value of the voxel, i.e. only those with value equal to 255. Therefore it is possible to easily describe multiple properties objects by setting multiple values for the voxel. For instance if we assume that a particular voxel value correspond to a particular material, we can describe, in addition to the geometry, also multiple mechanical properties. In this way a FE model can be generated so that its finite elements are already mechanically characterized.

The resulting *Nodes Coordinate Matrix* and *Finite Elements Connection Matrix* are general and can be read from any commercial FE software. The used method guarantees the matching of nodes and avoids any hypostatic circumstances as bad–linked elements.

Figure 4 illustrates the FE mesh obtained by appling the procedure to the structure represented in Figure 1. As it can be noticed, as long as the surface is regular and parallel to the axis directions, the resulting mesh precisely matchs the original geometry (Figure 4(a)), but when the surface is irregular (curved) or not planar to an axis direction, the resulting FE mesh is a jagged representation of the original geometry (Figure 4(b)). Despite this fact, it is always possible to improve the mesh accuracy using a smoothing method to reduce the faceting, see Figure 4(c). Concisely, these methods are linear low-pass filters that remove high curvatures variations (jag) and have to be chosen in order to not produce shrinkage, see for instance [14]. In what follows we do not use any of those procedures since we are interested in testing the raw procedure.

(a) External restitution   (b) Internal restitution   (c) Smoothed internal restitution

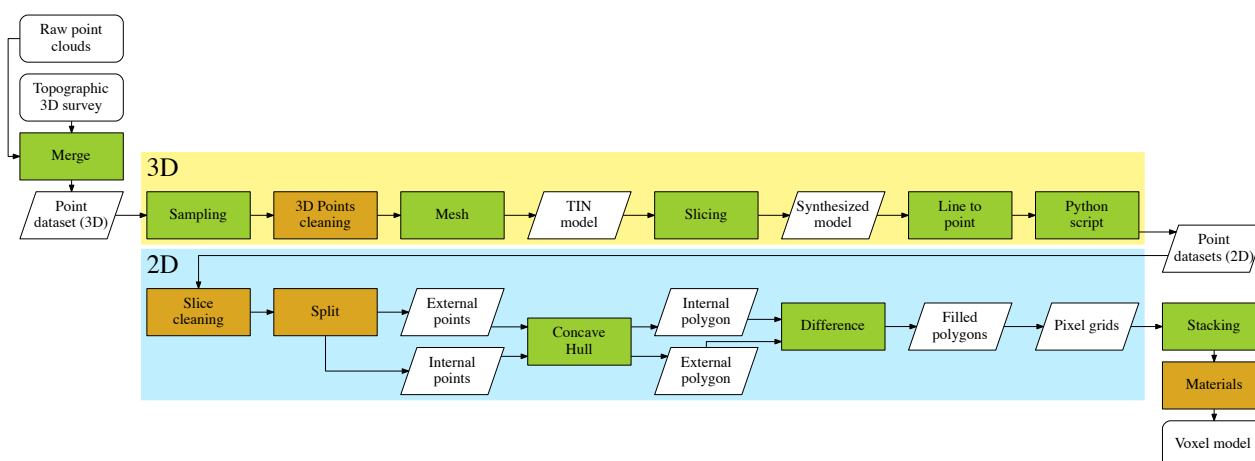**Figure 4.** Finite element mesh obtained by applying the procedure to the structure represented in Figure 1.

Figure 5. Flowchart for the proposed method: completely automated procedures (green) and semi-automated procedures (orange).

2.3. CLOUD2FEM conceptual workflow

The procedure previously described is synthesized in the flowchart of Figure 5. The input data are generic point clouds, merged into one single points data file for the whole building surveyed. The workflow begins with a 3D analysis divided into sequential steps. Most of the operations here described are completely automated (highlighted in green in the flowchart) using different algorithms. At the end of this first part, the building is described with a dataset of slices each containing bi-dimensional points. Each slice is then analyzed in a 2D environment, and this phase includes some semi-automatic analysis (highlighted in orange in the flowchart). All data are georeferenced using a unique local or global reference system, therefore final datasets are stackable. Each pixel grid, obtained from the corresponding slice, contributes to the creation of the voxel model.

3. Procedure Validation: the case of the San Felice sul Panaro Fortress

In order to validate and show the capabilities of the proposed technique, the case of the San Felice sul Panaro Fortress is presented and discussed.

3.1. The San Felice sul Panaro Fortress

The San Felice sul Panaro Fortress is a monumental historical building located in San Felice sul Panaro (Italy). It has been hit by the Emilia earthquake (2012) and it is object of several studies that aim to preserve its integrity [15]-[16]. As first intervention, the municipality of San Felice did a fine survey of the damaged building by using geomatic techniques, mainly laser scanning and photogrammetry, obtaining different products like point clouds, orthophotos, immersive visualization.

Here we focus the attention on the principal tower (Mastio) with the aim to extensively test the capabilities of this new technique. As shown in (Figure 6), the tower is composed by six layers of different kind: cross-vaults, wood slabs with old and remodelled structures. Each level is then characterized by irregular dimensions and thickness. By inspecting the South front illustrated in Figure 6(a) it appears how the seismic shock hit and damaged the tower by producing a lateral and torsional oscillation and residual displacements last on the actual configuration. Openings are placed irregularly on the structure and also have irregular shape and section (Figure 6(c) and Figure 6(d)). Summing up the structure is anything but regular.
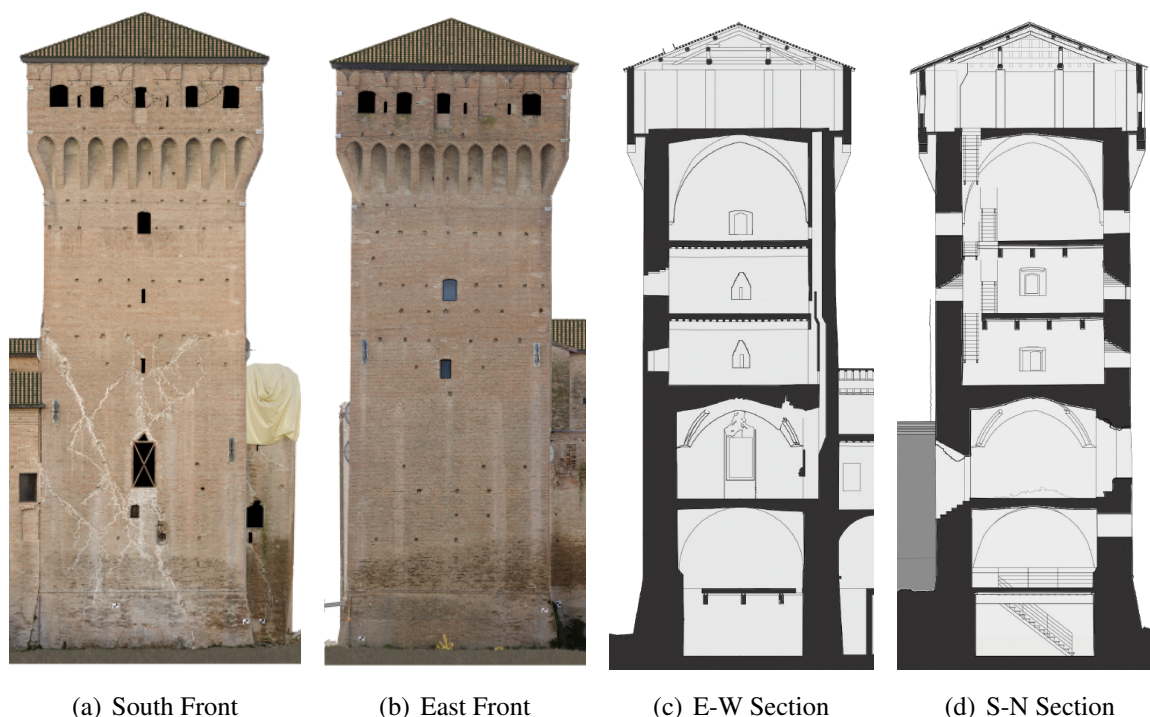

(a) South Front (b) East Front (c) E-W Section (d) S-N Section

Figure 6. San Felice sul Panaro Fortress Principal Tower.

3.2. Fortress Laser Scanner Survey and Slices Generation

In order to precisely capture the geometry of the San Felice sul Panaro Fortress, a total number of 163 scans were merged into a single cloud containing more than 40 million points. From this cloud a subset containing the points related to the Mastio has been extracted and analyzed, see Figure 7(a). As represented in Figure 7(b) the survey finely describes every single feature of the structure.

The point cloud has a very heterogeneous density, primarily related to the distance between the single scan positions and the object acquired. Figure 8(a) represents the points that are located within the range $[z_j - \Delta z/2, z_j + \Delta z/2]$, at a given z_j coordinate. In Figure 8(a) the lower left corner is magnified to show the original point cloud density.

In order to simplify this initial point cloud, a particular algorithm [17] was used to populate a new dataset with a point sampling generated according to a Poisson-disk distribution (*Sampling* procedure in Figure 5). The result was a new point cloud reduced to 3.2 million points, with a regular spatial sampling of 5 cm, suitable for further analysis.

It was then used a GIS software to manipulate the three-dimensional scanned data. The first operation was to clean the point cloud (*3D Points cleaning* in Figure 5), mainly removing all neighbors points not belonging to the building of our interest. In fact other surrounding buildings were acquired during the initial scan, in order to align all the different point clouds. These buildings can be removed from the point cloud, reducing it further down to 1.9 million points.

It must be considered the particular conditions of the tower. Regarding the exterior part of the model there were problems for the roofs partially collapsed, that was covered with large plastic tarpaulins in order to avoid water infiltration. Furthermore in the surroundings and in the internal courtyard of the building there was pile of rubble and debris. All these elements hide the actual geometry of the building from the laser scanner point of view. In fact in the three-dimensional point cloud these elements are acquired and then intrinsically fused with the proper model of the building and there is not an automatic procedure to perform a full cleaning in advance.

The point cloud is a three-dimensional model. However, it's necessary to build a model that consist of continuous surfaces (*Mesh* and *Polygonal Model* in Figure 5), through Triangular Irregular Network (TIN) mesh or Non-Uniform Rational B-Splines (NURBS) surfaces . In this study the polygon model has been realized using the TIN mesh (Figure 7(b)). Considering the points (x, y, z) in space, the conjunction between them is realized with lines forming adjacent triangles in order to represent the object with a continuous surface.

The mesh consisted in a total of 4.8 million triangles. It is a model that describes all the surfaces surveyed with the laser scanner, but it cannot be considered a correct *closed* model from the topological point of view, consider, for instance, the roof surface illustrated in Figure 7(a).

Regarding the interior part of the model we must account that at the moment of the laser scanner acquisition, there were furniture in different rooms, and also rubble and debris in some particular areas. Every disturbing element enhance the complexity of the building and they appear also in Figure 8(b).

By inspecting every single slice it appears very easy to find and properly clean every slice from points that do not belong to the building but have been inevitably acquired during the scanning. Using our procedure, by creating a concave hull that envelopes the internal points from the outside, the presence of internal debris or furniture located inside the room is irrelevant.
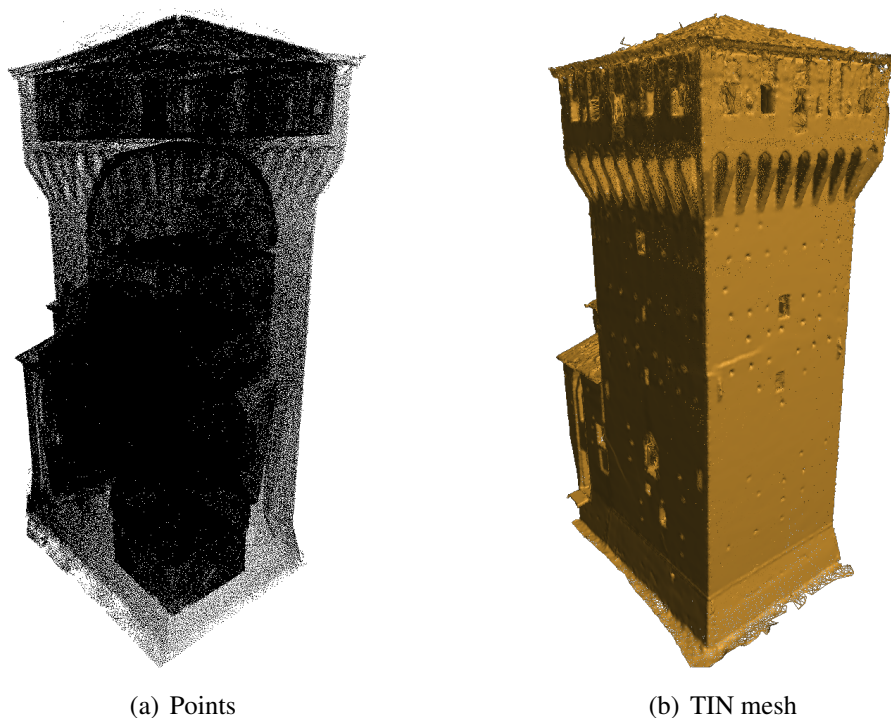
(a) Points (b) TIN mesh

Figure 7. Three-dimensional models for Mastio tower.

This part of the procedure is semi-automatic. We believe that some manual intervention is essential at this stage for an accurate separation between internal points and external points: this is especially true with data from complex buildings such as the one analyzed. The proposed workflow aims to minimize manual intervention in terms of time in order to maximize the efficiency of the procedure itself.
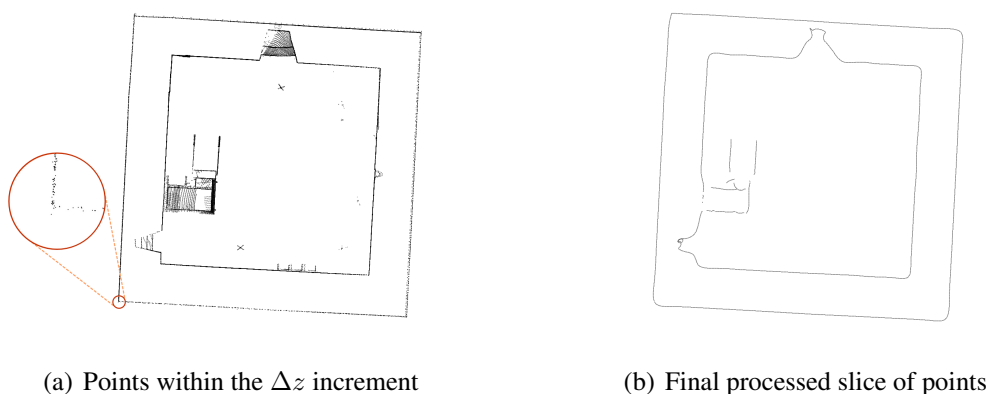

(a) Points within the Δz increment (b) Final processed slice of points

Figure 8. First part of the slicing workflow (3D data): the magnified portion shows the uneven density of the raw data

Based upon the Mastio geometry properties, we consider that a fine description of the tower can be done by slicing the tower height with a $\Delta z = 0.20$ meters that correspond, more or less, to three layers of bricks and two layers of mortar. On the other hand, the resolution of each slice is set to have $\Delta x = \Delta y = 0.115$ meters that correspond to the short dimension of the brick (half-brick).
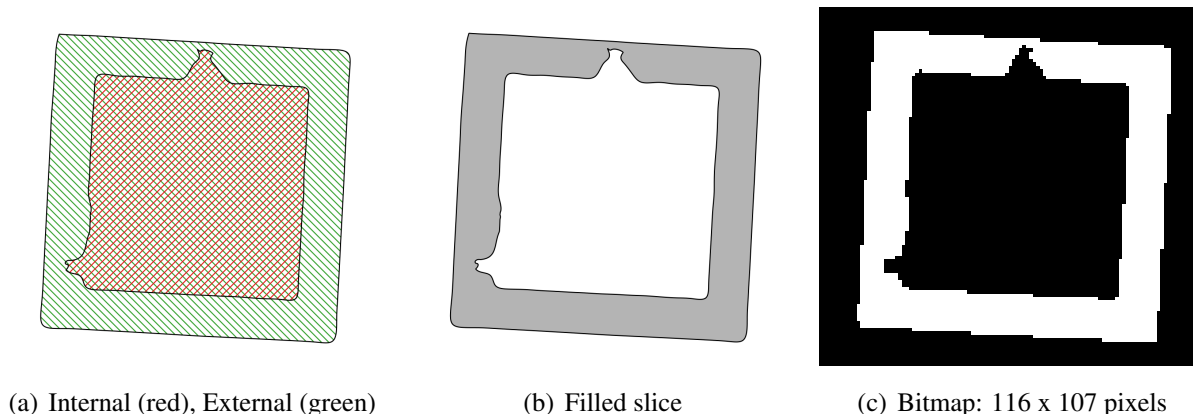
(a) Internal (red), External (green)   (b) Filled slice   (c) Bitmap: 116 x 107 pixels

Figure 9. Second part of the slicing workflow (2D data).

The resulting stacking sequence is composed by 153 horizontal slices, where each one is represented by a $N \times M$ grid of 116×107 pixels. Figure 8 and Figure 9 illustrate the i-slice representative of a generic section.

3.3. Mastio Finite Element Model Generation

Thanks to the material properties survey, the structure has been entirely described by using five different material property, whose mechanical properties are set according to [18] - [19], see Table 1. Figure 10 describes generic sections representation where the user can visualize and set the material properties based on his knowledge that may have acquired from direct inspection or available images. The resulting three-dimensional matrix is visualized by plotting its pattern by means of RGB colors in Figure 11.

Table 1. Mechanical characterization of materials by colors.

Material	Color	Elastic Modulus	Poisson's coeff.	Density
	$[0-255]$	$[MPa]$	$[-]$	$[kg/m^3]$
Masonry	255	1500	0.20	1800
Reinforced Masonry	150	1900	0.20	1800
Terrain	125	–	–	–
Timber	100	8000	0.37	415
Air	0	–	–	–

Voxels are plotted transforming row and column indexes to a unitary coordinate. Then the generation of the eight-nodes hexahedral FE model is done according to the instructions given in Figure 3 by associating their coordinates respectively to the Δx, Δy, Δz volume. It is important to notice that the three-dimensional matrix contains volumes for any arbitrary index (i, j, k) combination, i.e. values are assigned also to empty spaces (surrounding air, terrain, etc). The user can choose, according to the FE model purpose, to filter out some of the values. For instance, here, the voxels corresponding to the air and terrain properties are excluded by not being processed during the mesh generation procedure.

The final mesh is then characterized by 745,668 nodes and 661,105 elements, see Figure 12(a).
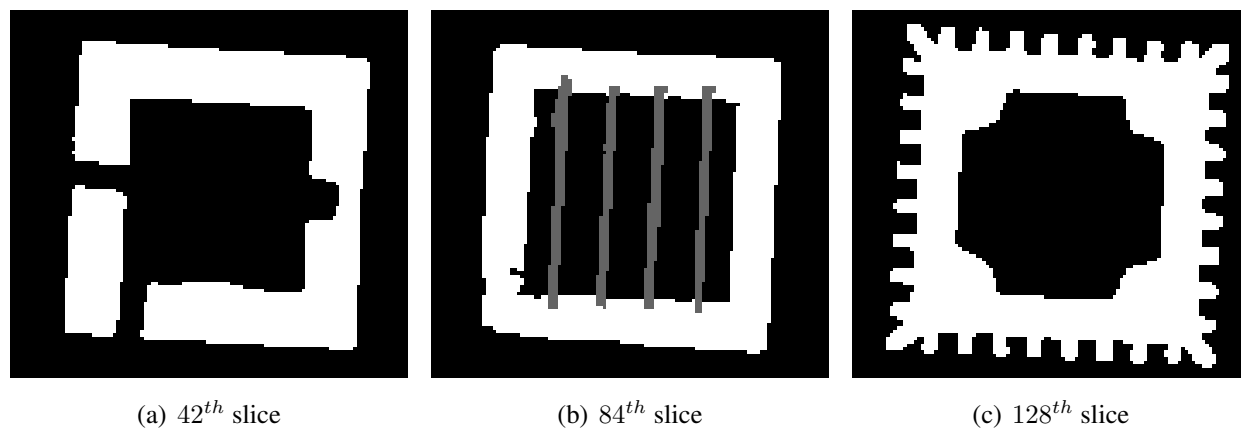

(a) 42th slice   (b) 84th slice   (c) 128th slice

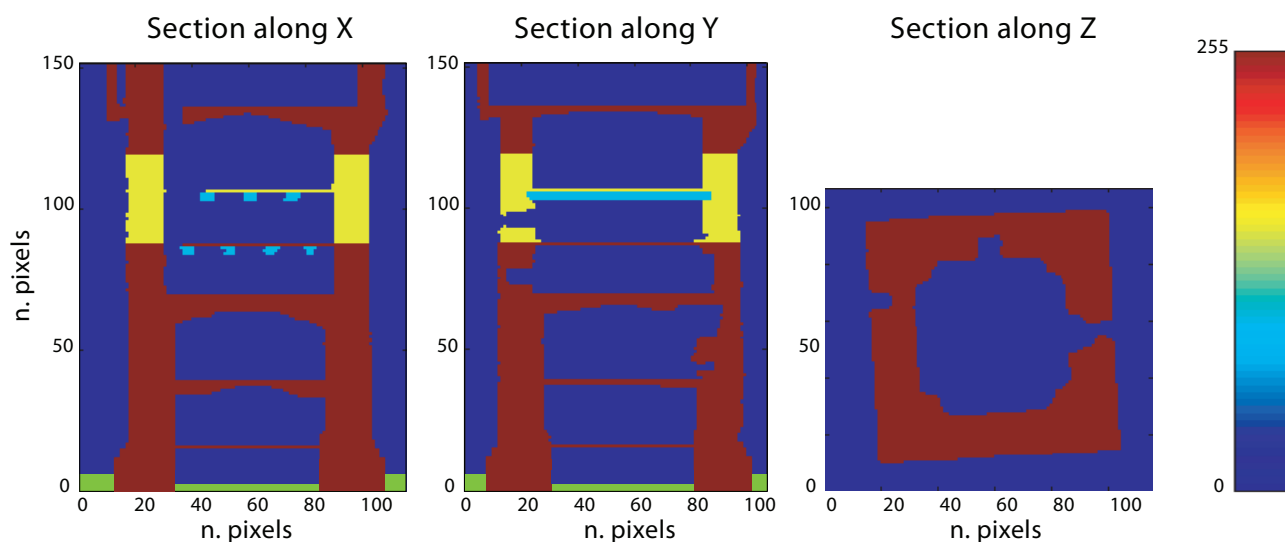**Figure 10.** Examples of bitmap slices.

Figure 11. Visualization of the three-dimensional material matrix: voxels possess unitary dimension. Color values are plotted according to Table 1. Compare the quality of details with sections illustrated in Figure 6(c)-6(d).
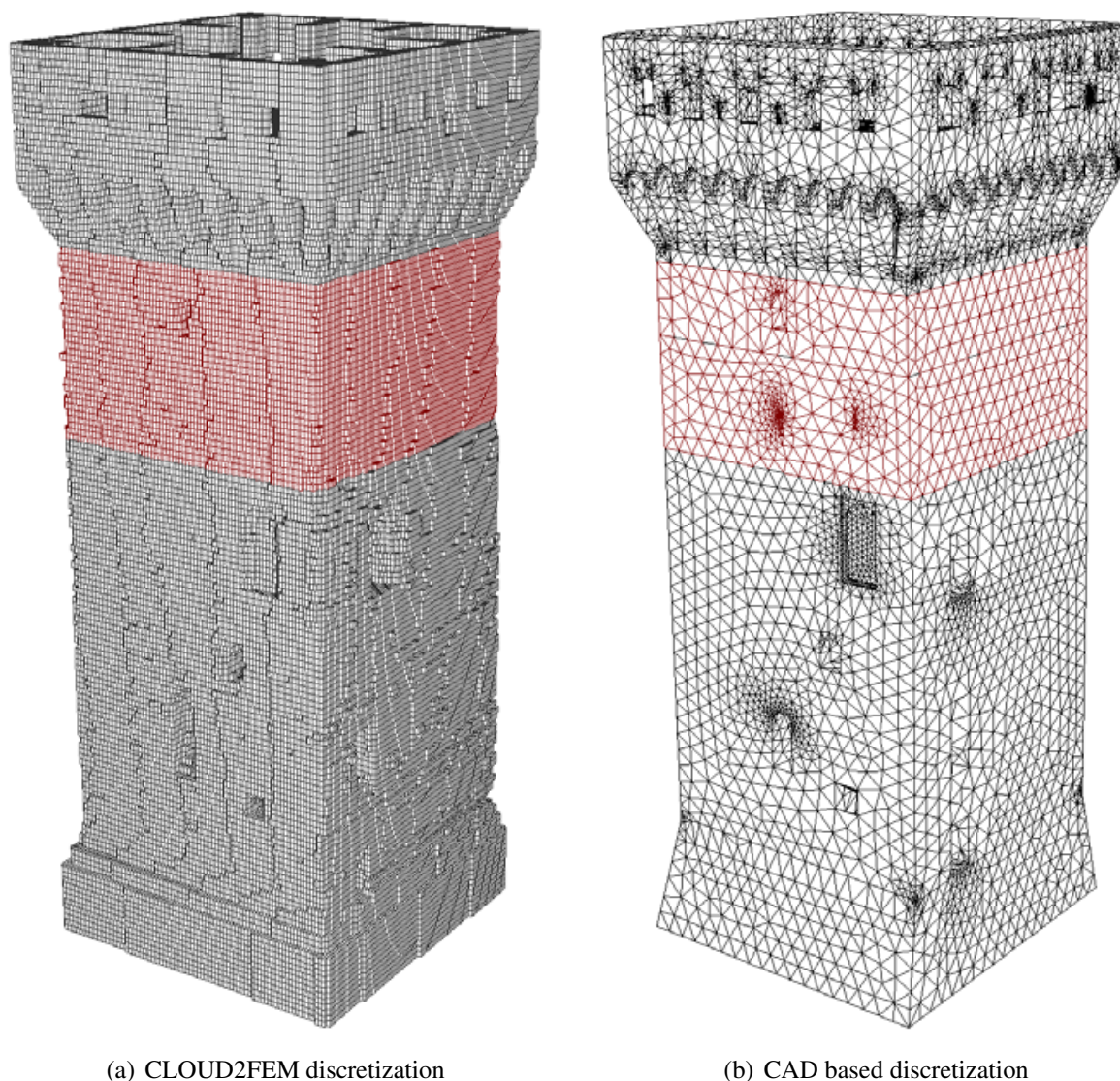
(a) CLOUD2FEM discretization   (b) CAD based discretization

Figure 12. Finite element discretization comparison - colors are set according to the material properties: gray and red colors are used to illustrate the masonry and the reinforced masonry elements respectively.

3.4. Structural Analysis and Comparison with CAD based model

Here the finite element model obtained by using the proposed procedure is tested within a structural analysis. A comparison is performed using a very accurate finite element model obtained by precise CAD procedure based upon the same laser scanner dataset, see Figure 12. The reference model [16] is obtained by means of tetrahedral four-node elements to model the masonry walls and four-node shell elements to model vaults and layers and counts 54,340 nodes and 215,938 elements.

In order to assess the accuracy of the proposed model, a linear natural frequency analysis (eigenvalue analysis) is performed. Clamped boundary conditions have been considered for nodes located at the ground level ($Z = 0$).

The Linear natural frequencies analysis is a common tool for the characterization of structures dynamic behavior. The *natural frequencies* and the *natural mode shapes of vibration*, which are characteristics of the structure, are given by the solution of the following eigenvalue problem:

$$\mathbf{K\Phi} = \lambda\mathbf{M\Phi}$$

where $\mathbf{M}$ is the mass matrix, $\mathbf{K}$ is the stiffness matrix, λ is an eigenvalue and $\mathbf{\Phi}$ is its relative natural mode shape of vibration (eigenvector). The eigenvalue problem does not fix the absolute amplitude of the vector $\mathbf{\Phi}$ but only its shape.

It is evident that both $\mathbf{M}$ and $\mathbf{K}$ are highly conditioned by the correct representation of the geometry and by the accurate mass and stiffness distribution along the structure. Table 2 summarize the computed mass and the overall dimensions for both the models. By inspecting Table 2 it is clear that the application of the proposed technique produces a finite element model which accurately describes the building geometry and its mass distribution.

Table 2. Mass, overall dimensions and center of mass height.

Model	Mass	Max dimensions	h_g
	$[ton]$	$\{L \times B \times H\}[m]$	$[m]$
CAD	3,055.78	$9.97 \times 9.97 \times 30.64$	13.67
Voxel	3,032.11	$9.90 \times 9.79 \times 30.60$	14.07

Table 3 collects the obtained results in terms of computed frequencies and computed errors. It appears that, for the first six modes the computed errors are always less than 4% and they are less than 0.1% for the 1st bending mode (*Fundamental mode*) in both directions (E-W and N-S).

We limited our discussion to the first six modes according to the structural meaning associated to the frequency and the corresponding mode shape. The tower dynamically acts as a cantilever beam whose fine description can be summarized by two bending modes in each horizontal direction plus a torsional mode and an axial mode.

Higher frequency modes are not compared since, expecially for masonry structures, they correspond to local modes: the assumption made by the user who conceives the model (i.e. the choice to employ shell elements to model layers or shell elements to model thin vaults, etc.) strongly characterize the local dynamic response.
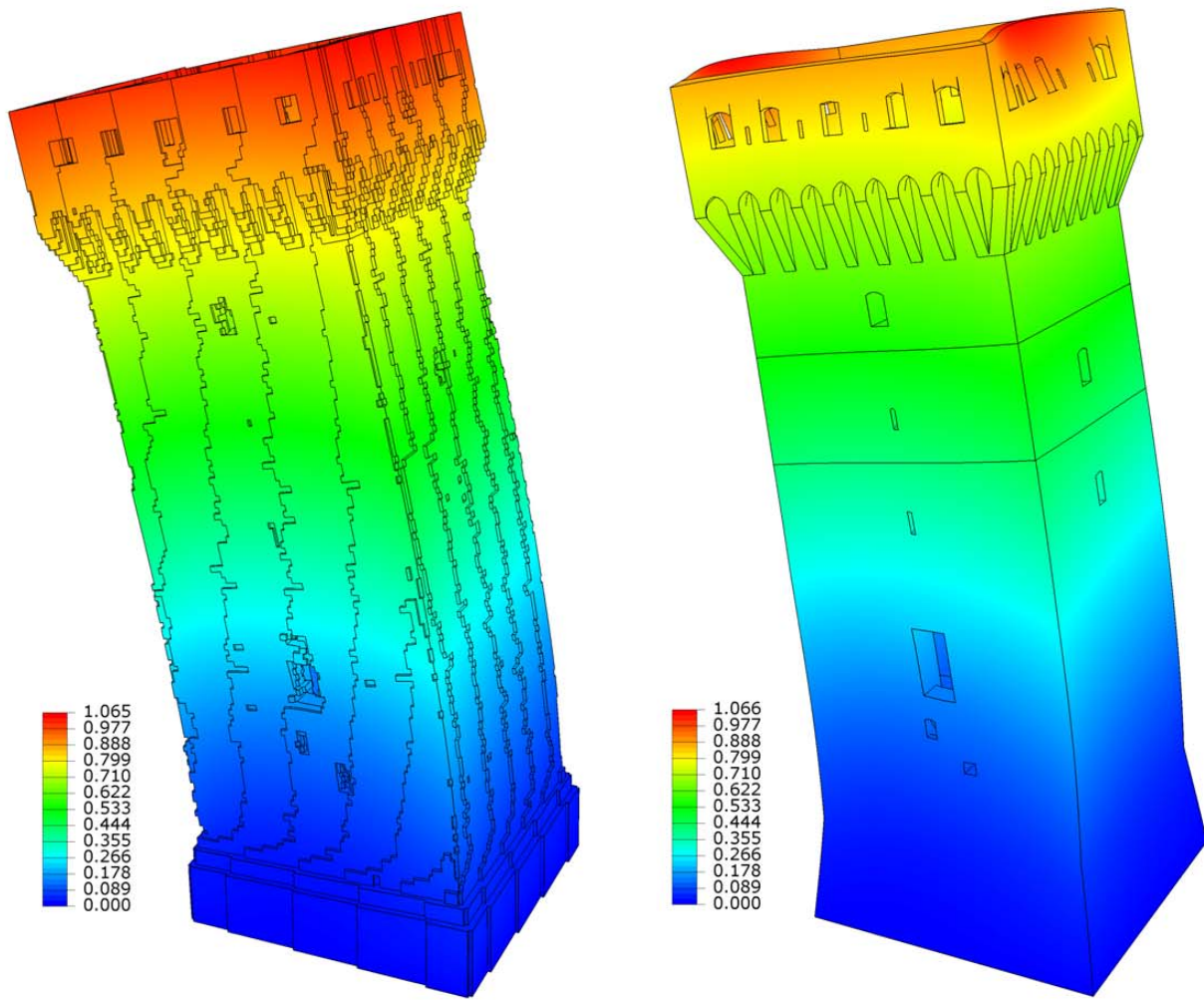
Figure 13 illustrates the mode shape n. 1 (*Fundamental mode*) where colors are associated to the magnitude of the computed amplitude (normalized). Mode shapes are in very good agreement for what concern the overall behavior and they slightly diverge for what concerne the local displacement distribution of the top part: in the CAD based model some simplistic assumption have been introduced on this specific part, due to the high geometry complexity. Some part of the structure have been considered adding to the model the corresponding mass values. On this regard the z coordinate of the center of mass has been computed for each model in order to check the overall mass distribution, see Table 2.

On the other hand the voxel based model captures every single detail of the geometry precisely, thanks to this semi–automatic procedure, avoiding the user interpretation or the necessity to *defeature* the complexity of the model. It has to be mentioned that the voxel model counts 2,237,004 degrees of freedom (dof) whereas the CAD model enumerates 163,020 dof.

An high computational cost seems to be accounted for because of the higher number of dof but in reality the overall user time is higher for the CAD based model. In fact if we consider the time needed to study and conceive the CAD geometry and the time spent to transfer the geometry into a FEM software (feature/defeature) we can determine a global required user time greater than the Voxel model one. Moreover, a more effective FE model prone to optimize the computational cost preserving accuracy might be obtained by coarsening the resolution of the voxels.

Table 3. Natural frequencies analysis: frequencies of the main mode shapes of the Mastio tower of the San Felice sul Panaro Fortress. Comparison between Voxel based model and CAD based model.

Mode #	Voxel Frequency (Hz)	CAD Frequency (Hz)	Error (%)	Mode description
1	1.9131	1.9137	0.031%	1st bending mode (E-W)
2	1.9276	1.9289	0.067%	1st bending mode (N-S)
3	4.5437	4.4253	2.675%	torsional mode
4	7.0804	7.3518	3.692%	2nd bending mode (E-W)
5	7.1654	7.3665	2.730%	2nd bending mode (N-S)
6	8.1623	8.0055	1.959%	axial mode

(a) Voxel freq. = 1.9131 Hz   (b) CAD freq. = 1.9137 Hz

Figure 13. Mode # 1: bending mode shape. Displacements magntiude.

4. Conclusions

A new technique, called *CLOUD2FEM*, to generate a FE model from a Laser Scanner survey of a complex building has been presented. In particular the structural validation of the Rocca San Felice Fortress Mastio FE model obtained using the mentioned procedure has been shown, thanks to a comparison analysis with a CAD based model. A very good agreement between the two models modal frequencies values has been obtained.

One of the strengths of the presented procedure is to be indipendent from any particular software.

It is worthy to underline that the voxel based model is composed only by eight-nodes hexahedral Finite Elements: problems caused by the matching of dofs of different element type (for example the connection between shell and brick elements) are avoided along with the user structural interpretation.

Moreover, if we calculate the global time spent in order to generate a complex structure FE model for both CAD based and *CLOUD2FEM* based procedures plus the computational time spent in the corresponding structural analysis, it is clear that with the proposed method there is an undeniable saving of user time. In addition, it should be emphasized that with our approach also users without advanced structural skills are able to complete the described analysis. We can assert that the proposed procedure is a speedy solution of a complex structure FE model generation problem.

Acknowledgments

Author Contributions

All authors have made significantly contributions to the paper. Giovanni Castellazzi and Antonio Maria D'Altri conceived the procedure and contributed for the coding related to the generation of FE models and for the validation using the structural analysis. Gabriele Bitelli, Alessandro Lambertini and Ilenia Selvaggi contributed for the processing of the TLS data and for the coding related to data optimization and data preparation for the FEM analysis.

Conflicts of Interest

The authors declare no conflict of interest.

References

1. Dorninger P. and Pfeifer N., A Comprehensive Automated 3D Approach for Building Extraction, Reconstruction, and Regularization from Airborne Laser Scanning Point Clouds *Sensors* **2008**, *8*, 7323-7343.
2. Africani, P.; Bitelli, G.; Lambertini, A.; Minghetti, A.; Paselli, E. Integration of LIDAR data into a municipal GIS to study solar radiation. *International Archives of the Photogrammetry, Remote Sensing and Spatial Information Sciences* **2013**, *XL-1/W1*, 1-6.

3. Chen, J.; Chen, B. Architectural Modeling from Sparsely Scanned Range Data. *International Journal of Computer Vision* **2008**, *78*, 223-236.

4. Guarnieri, A.; Pirotti, F.; Pontin, M.; Vettore, A. Combined three-dimensional surveying techniques for structural analysis applications. In Proceedings of the Third IAG, 12th FIG symposium, 2006.

5. Guarnieri, A.; Milan, N.; Vettore, A. Monitoring Of Complex Structure For Structural Control Using Terrestrial Laser Scanning (Tls) And Photogrammetry. *International Journal of Architectural Heritage* **2013**, *7*, 54-67.

6. Armesto, J.; Roca-Pardinas, J.; Lorenzo, H.; Arias, P. Modelling masonry arches shape using terrestrial laser scanning data and nonparametric methods. *Engineering Structures* **2010**, *32*, 607-615.

7. Lubowiecka, I.; Armesto, J.; Arias, P.; Lorenzo, H. Historic bridge modelling using laser scanning, ground penetrating radar andfinite element methods in the context of structural dynamics. *Engineering Structures* **2009**, *31*, 2667-2676.

8. Truong-Hong, L.; Laefer, D. Octree-based, automatic building facade generation from LiDAR data. *Computer-Aided Design* **2014**, *53*, 46-61.

9. Truong-Hong, L.; Laefer, D. Validating Computational Models from Laser Scanning Data for Historic Facades. *Journal of Testing and Evaluation* **2013**, *41*, 481-496.

10. Hinks, T.; Carr, H.; Truong-Hong, L.; et al. Point Cloud Data Conversion into Solid Models via Point-Based Voxelization. *Journal of Surveying Engineering* **2013**, *139*, 72-83.

11. Edelsbrunner, H.; Kirkpatrick, D.; Seidel, R. On the shape of a set of points in the plane. *IEEE Trans. Inf. Theory* **1983**, *29*, 551-559.

12. Moreira, A.; Santos, M.Y. Concave Hull: A k-Nearest Neighbours Approach for The Computation of The Region Occupied By A Set of Points. *Proceedings of the 2nd International Conference on Computer Graphics Theory and Applications (GRAPP 2007) Barcelona, Spain* **2006**, 61-68.

13. Castellazzi, G.; Krysl, P.; Rojas, L.; Cranford, T.W. Assessment of the effect of natural and anthropogenic aquatic noise on vaquita (Phocoena sinus) through a numerical simulation. *Advances in experimental medicine and biology* **2012**, *730*, 307-309.

14. Taubin, G. Curve and surface smoothing without shrinkage. In *ICCV '95*, Proceedings of the Fifth International Conference on Computer Vision, Cambridge, MA, USA, June 20-23th, 1995; IEEE Computer Society Washington, DC, USA 1995.

15. Cattari, S.; Degli Abbati, S.; Ferretti, D.; Lagomarsino, S.; Ottonelli, D.; Tralli, A. Damage assessment of fortresses after the 2012 Emilia earthquake (Italy). *Bulletin of Earthquake Engineering* **2014**, *12*, 2333-2365.

16. Orlando, A. Estense Fortress at San Felice Sul Panaro: modelling and seismic assessment. Master Thesis, Univestity of Genoa, Genoa, July 22th, 2014.

17. Corsini, M.; Cignoni, P.; Scopigno, R. Efficient and flexible sampling with blue noise properties of triangular meshes. *IEEE Transactions on Visualization and Computer Graphics* **2012**, *18*, 914-924.

18. NTC 2008, Norme Tecniche per le Costruzioni, D.M. 14/01/08, 2008.

19. Koponen, S.;Toratti, T.; Kanerva, P. Modelling elastic and shrinkage properties of wood based on cell structure. *Wood Science and Technology* **1991**, *25*, 25-32.

20. Rocca Estense di San Felice sul Panaro. www.roccaestense.dicam.unibo.it (accessed on 14 April 2015).